Ab initio investigation of the electronic structure and bonding properties of the layered ternary compound Ti_3SiC_2 at high pressure

2003 J. Phys.: Condens. Matter 15 1983

(http://iopscience.iop.org/0953-8984/15/12/315)

INSTITUTE OF PHYSICS PUBLISHING JOURNAL OF PHYSICS: CONDENSED MATTER

J. Phys.: Condens. Matter **15** (2003) 1983–1991 PII: S0953-8984(03)56147-1

Ab initio investigation of the electronic structure and bonding properties of the layered ternary compound Ti_3SiC_2 at high pressure

J Y Wang[1,2,3] **and Y C Zhou**[1]

[1] Shenyang National Laboratory for Materials Science, Institute of Metal Research, Chinese Academy of Sciences, Shenyang 110016, China
[2] International Centre for Materials Physics, Institute of Metal Research, Chinese Academy of Sciences, Shenyang 110016, China

E-mail: jywang@imr.ac.cn

Received 15 November 2002, in final form 18 February 2003
Published 17 March 2003
Online at stacks.iop.org/JPhysCM/15/1983

Abstract

The pressure dependences of the lattice parameters, electronic structure, and bonding properties of the layered ternary compound Ti_3SiC_2 were investigated by performing *ab initio* plane-wave pseudopotential total energy calculations. The material exhibited elastic anisotropy. The lattice constants and axial ratio were studied for different pressures, and the same trend was obtained as is measured in experiment. It was found that although the structure was stable at high pressure, the electronic structure and atomic bonding were definitely affected. The electrical conductivity was predicted to reduce with pressure, which was interpreted by analysing the band dispersion curve and density of states at the Fermi level. The strengths of the atomic bonds in Ti_3SiC_2 were considered by analysing the Mulliken population and by examining the bond length contraction for various pressures. A redistribution of charge density that accompanied high pressures was also revealed.

1. Introduction

The layered ternary carbides with a common formula of T_3MC_2, where T is a transition metal, M is an A-group (IIIA or IVA) element, and C is carbon, possess unique properties combining the merits of metals and ceramics, such as high thermal and electrical conductivity, low density, high strength and modulus, damage tolerance and thermal shock resistance, and being machinable [1]. The above significant properties derive from the layered crystal structure and the characters of the atomic bonding in Ti_3SiC_2: a mixture of metallic, covalent, and ionic

[3] Address for correspondence: Shenyang National Laboratory for Materials Science, Institute of Metal Research, Chinese Academy of Sciences, 72 Wenhua road, Shenyang 110016, China.

bonds are indicated by electronic structure calculations [2, 3]. Furthermore, by examining the distribution of charge density on the $(11\bar{2}0)$ plane of Ti_3AlC_2, Zhou *et al* [4] revealed that the titanium and carbon atoms formed strong directional Ti–C–Ti–C–Ti covalent bonding chains and that the pairs of these chains were linked by relatively weaker Ti–Al covalent bonds.

The mechanical properties and structural stability of Ti_3SiC_2 have been widely investigated in recent years, because of it being a structural material with promise for practical applications. Synchrotron x-ray diffraction measurements showed that Ti_3SiC_2 was structurally stable under pressure up to 61 GPa at room temperature [5]. *Ab initio* calculation was preliminarily used to calculate the elastic constants of Ti_3SiC_2 [6]. It was stated that the material is elastically isotropic, due to the close magnitudes of the second-order elastic constants c_{11} and c_{33}, as well as c_{12} and c_{13}, in the calculation.

It is known that the distribution of electronic density accompanying strain is responsible for a material's elastic properties [7]. Up to now, the relationship between the electronic structure and the elastic strain stability of this compound has remained far from being clarified. Hence, many properties of this group of compounds under high pressure are as yet unknown. By performing plane-wave pseudopotential total energy calculations in the present paper, we examined the changes of lattice parameters, bonding characters, and electronic structure that were induced by isotropic hydrostatic pressure.

2. Crystal structure and calculation method

Ti_3SiC_2 has a layered hexagonal crystal structure (space group D^4_{6h}–$P6_3/mmc$) and the atoms are located at the following Wyckoff positions: Ti at 2a and 4f, Si at 2b, and C at 4f. The unit cell of Ti_3SiC_2 used in the present computation is similar to that in previous work [8], in which the titanium atoms are indexed as Ti(1) (located at 2a positions) and Ti(2) (located at 4f positions), relating to the structurally non-equivalent positions.

We optimized the lattice parameters and calculated the ground-state electronic structure by using the standard CASTEP package. The CASTEP code is a plane-wave pseudopotential total energy calculation method that is based on density functional theory [9]. The electronic wavefunctions were expanded in a plane-wave basis set up to a 450 eV cut-off, which was sufficient for leading to good convergence for the total energy and the forces acting on the atoms. The norm-conserving pseudopotentials for Ti, Si, and C were generated using the optimized version of Kerker's scheme [10] and transformed into the separable form of the Kleinman–Bylander pseudopotential [11]. The electronic exchange–correlation energy was treated within the local density approximation scheme [12]. A Monkhorst–Pack mesh [13] of $8 \times 8 \times 2$ special $\boldsymbol{k}$-points for sampling was chosen in the calculations. The calculations of the partial density of states (PDOS) were performed using a projection of the plane-wave states onto a localized linear combination of atomic orbitals (LCAO) basis set. In the present case, the LCAO basis set consisted of the atomic pseudo-orbitals corresponding to the closed valence shell containing the valence electrons. According to this, the numbers of pseudo-orbitals were chosen as four for C, four for Si, and nine for Ti. Then the s, p valence orbitals of C were included in the calculation of the PDOS and the Mulliken population analysis, as well as s, p orbitals of Si or s, p, and d orbitals of Ti.

The external pressure was imposed upon the simulated unit cell as isotropic hydrostatic pressure. Calculations were performed for various pressures between 0 and 110 GPa, and the atomic configuration at zero pressure was referred to as the equilibrium state in this paper. The lattice parameters and internal atomic positions were fully optimized throughout the simulations until local minimizations of the total energy were realized.

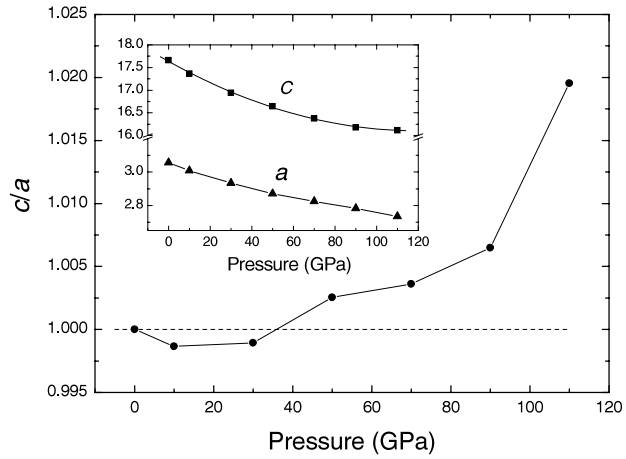

Figure 1. The pressure dependence of the calculated lattice constants and the corresponding axial ratio c/a of Ti_3SiC_2.

3. Results and discussion

3.1. Lattice parameters varying with pressure

To investigate the pressure dependence of the electronic structure and bonding properties of Ti_3SiC_2, geometrical configurations that possess the local minimum free enthalpy at each pressure are determined first of all. Figure 1 shows the calculated lattice constants and axial ratio c/a varying with pressure. It is seen that the a- and c-axis lengths contract to different extents with increasing pressure, as shown in the inset of figure 1. The a-axis length decreases almost linearly with increasing pressure, while the trend obtained for the c-axis exhibits a parabolic curve-like shape over the whole pressure region. The calculated relationship between the c-axis length and pressure can be fitted by a second-order polynomial. The c/a axial ratio is plotted in figure 1 as a function of external pressure. The c/a ratio is smaller than the equilibrium value when the pressure is less than about 30 GPa. Subsequently, it increases monotonically with increasing pressure. The c/a ratio is significantly greater than that of the equilibrium configuration beyond 50 GPa.

The above results reveal that the compound is basically elastically anisotropic over the whole pressure range simulated. The material is slightly softer in the direction that is perpendicular to the basal plane than in the parallel direction when the external pressure is less than 30–40 GPa, but it is stiffer in the direction that is perpendicular to the basal plane than in the parallel direction when the pressure is over 50 GPa. The present results agree well with experimental observations of the pressure dependence of the lattice parameters [5].

We also studied the relative change of unit-cell volume, V/V_0, as a function of external pressure. By fitting the Birch–Murnaghan equation of state [5], the bulk modulus B_0 and its pressure derivative B_0' were obtained as 196 GPa and 3.9, respectively. These values were comparable with experimental results: $B_0 = 206 \pm 6$ GPa and $B_0' = 4.0 \pm 0.3$ [5].

3.2. Pressure dependence of the bonding properties

Zhou *et al* [4] considered the different covalent bonding strengths in Ti_3AlC_2 by examining bond lengths in the equilibrium state. The results showed that the Ti(1)–C and Ti(2)–C bond

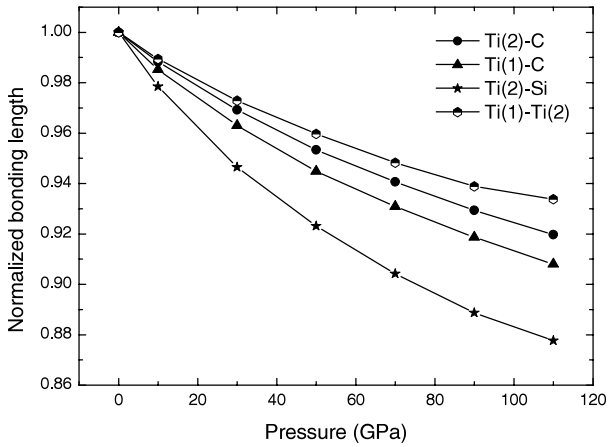

Figure 2. Normalized bond lengths in the Ti_3SiC_2 unit cell as a function of pressure.

lengths in layered compounds were not equal. Owing to the close relationship between the crystal structures of Ti_3SiC_2 and TiC [14], the Ti(1)–C and Ti(2)–C bond lengths are usually compared with that of Ti–C in TiC to demonstrate the degree of covalent bonding. The present calculated Ti–C bond length (2.168 Å) in the equilibrium state of TiC is very close to the experimental value (2.165 Å) [15], and correctly located between the lengths of the Ti(1)–C (2.181 Å) and Ti(2)–C (2.094 Å) bonds in Ti_3SiC_2. It is also interesting to examine the lengths of Ti–C bonds in TiC and Ti_3SiC_2 at different pressures. As an example, we just illustrate the Ti–C bond length contraction in both compounds at a pressure of 50 GPa. The bond length contractions, which were obtained by normalizing the bond length by the equilibrium value, are 0.950 for the Ti–C bond in TiC, and 0.945 for Ti(1)–C and 0.953 for Ti(2)–C in Ti_3SiC_2. This shows that the Ti(2)–C bonding is stiffer and the Ti(1)–C bonding is softer than the Ti–C bonding in TiC.

By comparing the magnitude of the contraction of the bond lengths and examining the degradation of atomic bonds at various pressures, we can evaluate the bonding strengths in Ti_3SiC_2. In the first instance, we show the bond length contraction against various pressures in figure 2. The lowest-lying curve for Ti(2)–Si indicates that it is the most compressible covalent bond. Above it are located Ti(1)–C and Ti(2)–C, in that order, and then the Ti(1)–Ti(2) ionic bonding. For example, the bond length of Ti(2)–Si decreases to 87.7% when pressure increases to 110 GPa, while the corresponding values are 90.81% for Ti(1)–C, 91.98% for Ti(2)–C, and 93.4% for Ti(1)–Ti(2). This shows that the Ti(1)–C and Ti(2)–C bonds are stronger than Ti(2)–Si, and Ti(1)–Ti(2) shows the stiffest bonding.

Mulliken population analysis has long been used to indicate the degree of covalency in materials, and it has been successfully combined with *ab initio* plane-wave electronic structure calculations [16] recently. A positive population means that atoms are bonded, while a negative value indicates anti-bonded states. We list the relative changes in population $\Delta\mathrm{BO}(p)$ for covalent and ionic bonds in Ti_3SiC_2 at various pressures in table 1. The values of $\Delta\mathrm{BO}(p)$ are obtained as follows:

$$\Delta\mathrm{BO}(p) = (\mathrm{BO}(p) - \mathrm{BO}(0))/\mathrm{BO}(0) \tag{1}$$

where BO(0) is the population at zero pressure and BO(p) is the value at pressure p. According to the definition, negative $\Delta\mathrm{BO}(p)$ represents weakening of the covalent bonding, and a positive value corresponds to strengthening. Table 1 shows that all types of covalent bond are weakened

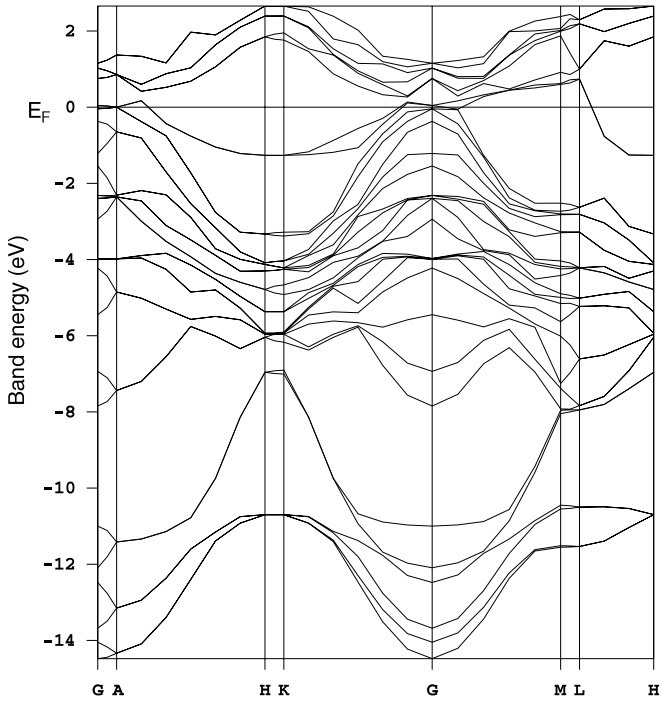

Figure 3. Band dispersion curves along some high-symmetry directions in the BZ for Ti_3SiC_2 at 110 GPa.

at high pressure. The populations are decreased by about 42.1% for the Ti–Si bond, 13.1% for the Ti(1)–C bond, and 3.5% for the Ti(2)–C bond, when the pressure is increased to 110 GPa. This result coincides with that discussed in analysing the bond length variation with pressure. Previous work showed that the ionic bonding characteristic arose from the charge transfer from Ti to the A and X atoms in the layered ternary compounds $Ti_{n+1}AX_n$ [4]. The Ti(1) and Ti(2) atoms possess positive effective charge and repel each other strongly when the lattice parameters are contracted due to pressure. The repulsive ionic bonding between Ti(1) and Ti(2) atoms is increased by a factor of about 1.5 in magnitude with pressure increasing to 110 GPa.

3.3. Electronic structure at high pressure

Electronic structures, as represented by e.g. the band dispersion curve and the density of states (DOS), at different pressures are investigated in this section. In most cases, we compare the results for Ti_3SiC_2 at a pressure of 110 GPa with those for the equilibrium state.

Figure 3 shows the band dispersion curves along some high-symmetry directions in the Brillouin zone for Ti_3SiC_2 at 110 GPa. It shows that the valence and conduction bands are still overlapping near the Fermi level. This indicates that the electrical conducting property of Ti_3SiC_2 could be preserved at high pressure. But the overlapping characters near the Fermi level are evidently influenced by pressure. The overlaps are along the G–M and G–K directions which are parallel to the basal plane for the equilibrium state of Ti_3SiC_2. When the pressure is increased to 110 GPa, the overlapping along the G–K direction vanishes, and that along G–M is also diminished. This implies that the electrical conductivity of Ti_3SiC_2 would be

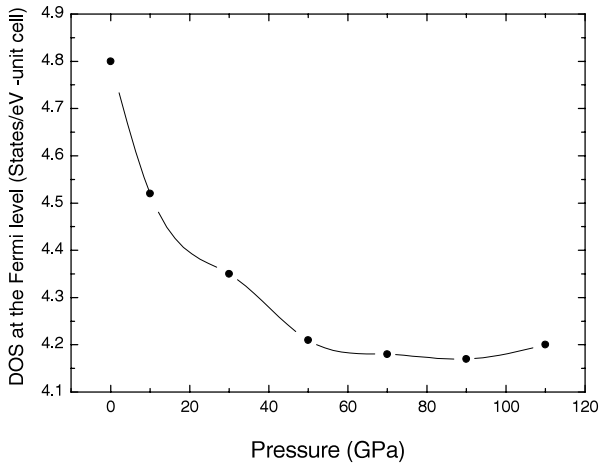

Figure 4. The pressure dependence of the total DOS at the Fermi level.

Table 1. Mulliken population analysis of the atomic bonds in Ti_3SiC_2 at high pressures.

Pressure (GPa)	Ti(2)–C (%)	Ti(1)–C (%)	Ti(2)–Si (%)	Ti(1)–Ti(2) (%)
20	0	−3.6	−4.0	19.1
50	0	−8.3	−15.8	60.0
70	0	−10.7	−22.4	94.2
90	−0.7	−13.1	−28.9	130.8
110	−3.5	−13.1	−42.1	161.7

decreased under pressure. It should also be noted that in figure 3 the Si 3s band overlaps with higher-energy bands along the M–L direction at about −8 eV.

The high electric conductivity of Ti_3SiC_2 has already been interpreted on the basis of the metallic bonding characters near the Fermi level [8]. By comparing the total density of states (TDOS) per unit cell at different pressures, we find that the DOS at the Fermi level ($N(E_F)$) is obviously affected by pressure. We further plot $N(E_F)$ as a function of pressure in figure 4. This figure shows that $N(E_F)$ decreases rapidly when pressure increases from zero to about 50 GPa, and tends to saturation at a constant value beyond 50 GPa. In order to interpret the intrinsic physical nature of the $N(E_F)$ reduction, it is worth examining the projected PDOS for the different types of atom in Ti_3SiC_2.

The PDOS of the atoms in the equilibrium configuration of Ti_3SiC_2 have been shown before [2, 8]. The lowest valence states for Ti(1) and Ti(2) overlapped with the C 2s state at around −12.5 to −9.0 eV. The electronic states below the Fermi level were dominated by strong p–d bonding between Ti 3d and C 2p (or Si 3p) states. The d-band bonding peaks of Ti(1) and Ti(2) were well separated from anti-bonding states by two non-bonding peaks that are located near the Fermi level. This indicates that the metallic properties mainly arise from the nearly free electronic states of (001)-like Ti monolayers in Ti_3SiC_2.

Figure 5 shows the PDOS for Ti_3SiC_2 at 110 GPa. It is seen that, although typical features of the covalent bonding in Ti_3SiC_2 are preserved, some distinct differences can be observed. The Si 3s and Si 3p states exhibit a higher level of s–p hybridization in the region around −13.6 to −6.0 eV. The widths of the lowest-lying peaks of Ti(1, 2) are changed from 3.5 to 4.5 eV

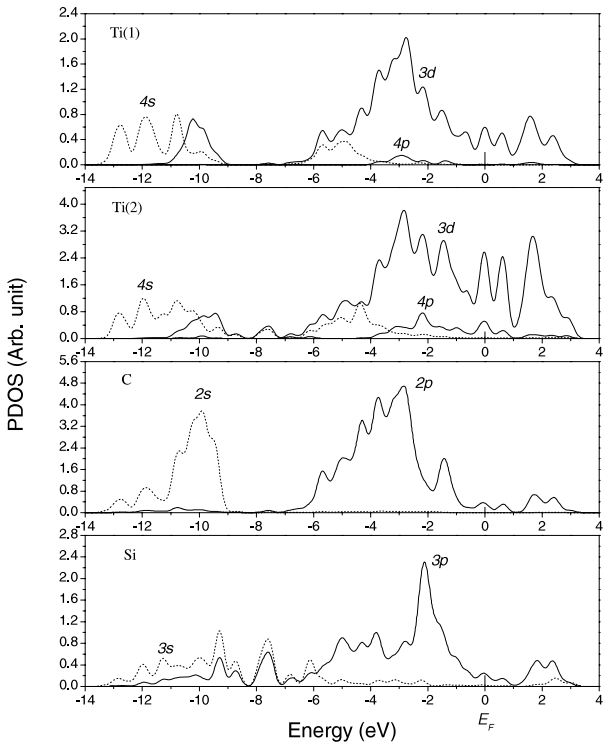

Figure 5. PDOS of Ti(1), Ti(2), Si, and C atoms at 110 GPa.

due to lattice constant contraction. One of the most interesting points is the appearance of new peaks in figure 5, which are located near to and above the Fermi level. In order to understand the origin of these peaks, we compared them with PDOS peaks in the same energy region of bulk Ti, and found that they were rather similar. This leads to the conclusion that the (001)-like Ti monolayer exhibits electronic properties more analogous to those of pure elemental bulk Ti. Unfortunately, this results in a reduction of the electrical conductivity for Ti_3SiC_2. Previous work showed that the layered ternary compounds were good electrical conductors as a class. The room temperature electrical conductivity of Ti_3SiC_2 was about four times that of pure Ti [17]. This means that the more similar the electronic states of Ti(1, 2) atoms are to those of bulk Ti, the greater the decrease in the electrical conductivity under pressure observed for Ti_3SiC_2.

3.4. Bonding charge density analysis

The mechanical strength of materials is due ultimately to the atomic bonding strength, and strain always involves charge density redistribution along certain directions. As regards the present work, although the essentials of the atomic bonding are preserved for Ti_3SiC_2 up to high pressure, the redistribution of the charge density still needs to be investigated; it will be helpful in understanding the intrinsic character of the phase stability for Ti_3SiC_2 under isotropic hydrostatic pressure. The bonding charge density $\Delta\rho(\vec{r})$ is defined as the difference between the total charge density $\rho_{comp}(\vec{r})$ in the compound and the electron density of overlapping free

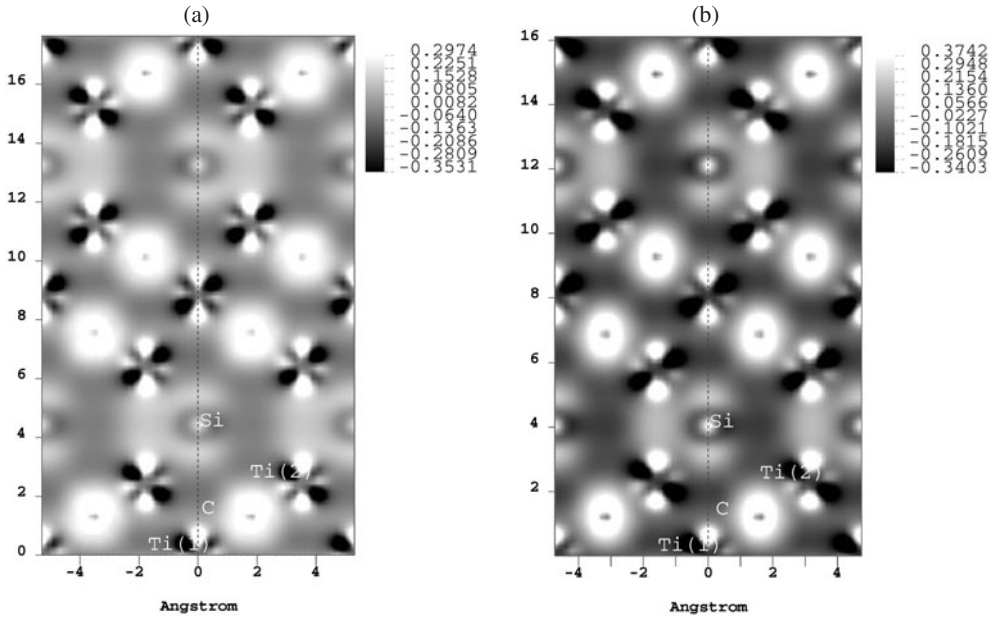

Figure 6. The bonding charge density on the $(11\bar{2}0)$ plane of Ti_3SiC_2 for pressures of (a) zero and (b) 110 GPa.

atoms $\rho_{ofa}(\vec{r})$, i.e.

$$\Delta\rho(\vec{r}) = \rho_{comp}(\vec{r}) - \rho_{ofa}(\vec{r}). \tag{2}$$

Positive $\Delta\rho$ means a surfeit of electron density, while a negative value indicates depletion of the electron density.

We plot the bonding charge densities on a slice of the $(11\bar{2}0)$ plane in figures 6(a) and (b) for pressures of zero and 110 GPa, respectively. The $(11\bar{2}0)$ plane contains Ti, Si, and C atoms and can represent the characteristics of covalent and ionic bonds in Ti_3SiC_2. Figure 6(a) demonstrates that the accumulation of charge density at C and Si sites is accompanied by significant anisotropic redistribution of d-state charge density at Ti sites. The surfeit of charge density for Ti atoms is not along the nearest Ti–C covalent bond chain. On the other hand, charge density transfers along the *c*-axis direction and increases slightly along the basal plane. The depletion of the charge density is in the direction that is perpendicular to the nearest Ti–C covalent bonding. The bonding charge density is rather spherical in shape on the C site, and it exhibits typical characteristics of p–s hybridization on the Si site.

When the solid was subjected to a pressure of 110 GPa, charge density transfer could be observed (see figure 6(b)). More charge density is accumulated at C and Si sites, which indicates that the effective charges of C and Si atoms are increased and the ionic bonding becomes stronger at high pressure. It is also found that the distribution of bonding charge density of the C atom is extended in the *c*-direction, and more charge density is transferred to the 3d–p_z state of the Ti atom. Figure 6(b) demonstrates that the bond directionality becomes larger, and no shear distortion of the bonding charge density (that may cause structural transition) is observed in Ti_3SiC_2 at high pressure. This may be the intrinsic reason for the structural stability for Ti_3SiC_2 at high pressure.

4. Conclusions

We have investigated the pressure dependence of the lattice parameters, electronic structure, and bonding characters of Ti_3SiC_2 by means of *ab initio* plane-wave pseudopotential total energy calculations. The compound Ti_3SiC_2 exhibits elastic anisotropy over the whole pressure range investigated. The electronic structure and atomic bonding are evidently affected by pressure. A trend of decrease of the electrical conductivity with increasing pressure is predicted. By performing Mulliken population analysis and examining the bond length contraction at various pressures, the Ti–Si bond is demonstrated to possess the weakest covalent bonding strength; above it are located Ti(1)–C and Ti(2)–C, and the ionic repulsive Ti(1)–Ti(2) bonding is the stiffest in Ti_3SiC_2. A characteristic of charge density redistribution that accompanies high pressures is also revealed.

Acknowledgments

This work was supported by the National Outstanding Young Scientist Foundation (Y C Zhou) under Grant No 59925208, the Natural Sciences Foundation of China under Grants No 50232040, No 50171071 and No 90206044, the '863' project, and the High-Tech Bureau of the Chinese Academy of Sciences. J Y Wang would like to thank Dr Q M Hu for helpful discussions.

References

[1] Barsoum M W 2000 *Prog. Solid State Chem.* **28** 201
[2] Medvedeva N I, Novikov D L, Ivanovsky A L, Kuznetsov M V and Freeman A J 1998 *Phys. Rev.* B **58** 16042
[3] Ahuja R, Eriksson O, Wills J M and Johansson B 2000 *Appl. Phys. Lett.* **76** 2226
[4] Zhou Y C, Wang X H, Sun Z M and Chen S Q 2001 *J. Mater. Chem.* **11** 2335
[5] Onodera A, Hirano H, Yuasa T, Gao N F and Miyamoto Y 1999 *Appl. Phys. Lett.* **74** 3782
[6] Holm B, Ahuja R, Li S and Johansson B 2001 *Appl. Phys. Lett.* **79** 1450
[7] Eberhart M E, Clougherty D P and MacLaren J M 1993 *J. Mater. Res.* **8** 438
[8] Zhou Y C, Sun Z M, Wang X H and Chen S Q 2001 *J. Phys.: Condens. Matter* **13** 10001
[9] Payne M C, Teter M P, Allan D C, Arias T A and Joannopoulos J D 1992 *Rev. Mod. Phys.* **64** 1045
[10] Lin J S, Qteish A, Payne M C and Heine V 1993 *Phys. Rev.* B **47** 4174
[11] Kleinman L and Bylander D M 1982 *Phys. Rev. Lett.* **48** 1425
[12] Perdew J P and Zunger A 1981 *Phys. Rev.* B **23** 5048
[13] Monkhorst H J and Pack J D 1976 *Phys. Rev.* B **13** 5188
[14] Zhou Y C and Sun Z M 2000 *Mater. Res. Innovat.* **3** 286
[15] Jeitschko W, Nowotny H and Benesovsky F 1964 *J. Less-Common Met.* **7** 133
[16] Segall M D, Shah R, Pickard C J and Payne M C 1996 *Phys. Rev.* B **54** 16317
[17] Sun Z M and Zhou Y C 1999 *Phys. Rev.* B **60** 1441